CRYSTAL STRATIGRAPHY OF TWO BASALTS FROM APOLLO 16: UNIQUE CRYSTALLIZATION OF PICRITIC BASALT 60603,10-16 AND VERY-LOW-TITANIUM BASALT 65703,9-13.

P. H. Donohue*[1], C. R. Neal*[1], R. E. Stevens[2], and R. A. Zeigler[3], [1]Civil & Environmental Engineering & Earth Sciences, University of Notre Dame, Notre Dame, IN (*NASA Lunar Science Institute; pdonohu1@nd.edu; neal.1@nd.edu) [2]University of Leicester, Leicester, UK [3]NASA Johnson Space Center, Houston, TX.

Introduction: A geochemical survey of Apollo 16 regolith fragments found five basaltic samples from among hundreds of 2-4 mm regolith fragments of the Apollo 16 site [1]. These included a high-Ti vitrophyric basalt (60603,10-16) and one very-low-titanium (VLT) crystalline basalt (65703,9-13). Apollo 16 was the only highlands sample return mission distant from the maria (~200 km). Identification of basaltic samples at the site not from the ancient regolith breccia indicates input of material via lateral transport by post-basin impacts. The presence of basaltic rocklets and glass at the site is not unprecedented (e.g., [2-4]), and is required to satisfy mass-balance constraints of regolith compositions [1,5]. However, preliminary characterization of olivine and plagioclase crystal size distributions indicated the sample textures were distinct from other known mare basalts, and instead had affinities to impact melt textures [6].

Impact melt textures can appear qualitatively similar to pristine basalts, and quantitative analysis is required to distinguish between the two in thin section [7-10]. The crystal stratigraphy method is a powerful tool in studying of igneous systems, utilizing geochemical analyses across minerals and textural analyses of phases. In particular, trace element signatures can aid in determining the ultimate origin of these samples and variations document subtle changes occurring during their petrogenesis.

Methods: Major and minor mineral analyses, back scatter electron images, and x-ray maps were made on the JEOL JXA 8200 electron microprobe at the University of Washington in St. Louis (St. Louis, MO). Quantitative mineral analyses (feldspar, pyroxene, olivine, Ti-oxide, and glass) were made by wavelength-dispersive x-ray spectrometry. Mineral compositions were measured at an accelerating potential of 15 KV, a beam current of 25 nA, an electron beam spot size of 1-20 μm, and 30-second count time for each element. Analyses were obtained using the Probe for EPMA software, with typical count times of 30 sec on peak and 20-30 sec on backgrounds. The measurements were quantified using the Armstrong PRZ algorithm coupled with Henke and Heinrich mass absorption coefficients [11].

Trace element analyses were made using an Element2 ICP-MS coupled to a UP213 ND:YAG laser ablation system at the University of Notre Dame Midwest Isotope and Trace Element Research Analytical Center (MITERAC; Notre Dame, IN). A 5 Hz repetition rate resulted in ~10-15 J/cm^2 fluence for 15-60 μm beam sizes dependent on crystal size. CaO was the internal standard for silicates (feldspar, pyroxene, olivine) and glass, and TiO_2 was utilized for Ti-oxides. The external standard for olivine (NIST SRM 610 glass) and plagioclase and matrix glass (NIST SRM 612 glass) are recognized in the analytical community [12]. Ilmenite laths in 60603,10-16 were too small and skeletal for LA-ICP-MS analysis. Data were reduced using the *GLITTER*® software [12], which allows for time-resolved background (~50 seconds) and signal (~60 seconds) selection. Signal review was used to monitor for accidental cracks, inclusions or adjacent phase analysis, and no such influences were found in the analyses.

VLT fragment 65703,9-13: The majority of sampled impact melts and impact melt breccias formed in basin-scale impacts into a highly feldspathic crust. Basin-sized impacts would likely form a melt with a unique cooling rate and crystallization history relative to smaller-scale impacts. Impact melting of a highly feldspathic target material may also lead to an initial oversaturation of plagioclase in the impact melt, with correspondingly high initial nucleation density. The plagioclase CSD of 65703,9-13 presented in [6] was ambiguous, and could be explained by extending either the impact melt field or basalt field.

Mineral compositions were obtained to resolve this ambiguity. Plagioclase compositions of Apollo 14 basalts reflect the KREEP signature in the source with a spread in La/Y and low Sr (ppm) in Fig. 1. In contrast, pristine basalts from Apollo 12 and Apollo 17 have a low La/Y values with less variation than plagioclase in Apollo 14 basalts and impact melts. Plagioclase in 65703,9-13 has a low La/Y ratio, with low overall Sr and La (Fig. 1).
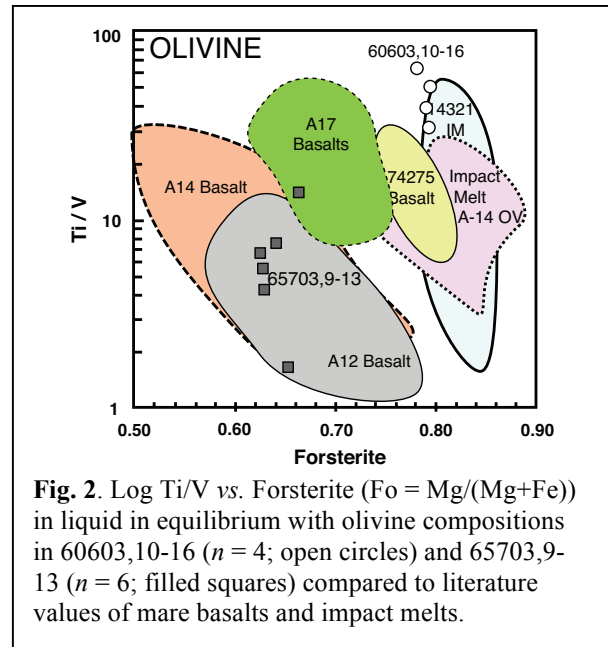
Picritic fragment 60603,10-16: Olivines that crystallized from an impact melt are compositionally distinct from mare basalt olivine [8]. Relative to mare basalts, impact melt olivines were found to contain generally higher forsterite content (Fo_{87-79}), and lower Mn (750-1800 ppm) and Co (~50-20 ppm), and higher Ti/V ratio for a given Fo-value [8]. Olivines in 60603,10-16 have high Fo_{79-78} and a high Ti/V ratio of 30 to 63 (Fig. 2), while Mn and Co abundance is similar to mare basalts (Table 1). In their investigation of impact melt breccias and olivine vitrophyres from the
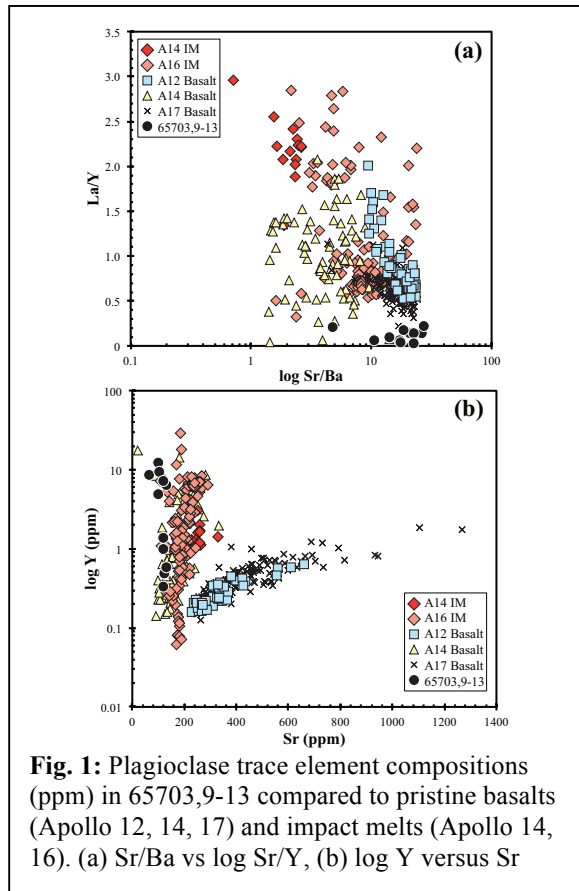
Fig. 1: Plagioclase trace element compositions (ppm) in 65703,9-13 compared to pristine basalts (Apollo 12, 14, 17) and impact melts (Apollo 14, 16). (a) Sr/Ba vs log Sr/Y, (b) log Y versus Sr

Fig. 2. Log Ti/V *vs.* Forsterite (Fo = Mg/(Mg+Fe)) in liquid in equilibrium with olivine compositions in 60603,10-16 ($n = 4$; open circles) and 65703,9-13 ($n = 6$; filled squares) compared to literature values of mare basalts and impact melts.

Apollo 14 site, [8] suggested either a) impact melting processes resulted in high-Fo, high-Ti/V olivine compositions, or b) some Apollo 14 impact melts originated in a high-Ti source region. In particular, the authors noted the tendency for olivines from Type C basalt 74275 to fall within the impact melt field (Fig. 2). This may instead result from inherent high-Ti in the source magma. This magma would be closer in composition to the picritic source, which would influence the initial olivine composition. We therefore suggest the olivine-impact melt discrimination method proposed by [8] only applies for low-Ti mare basalts and impact melts and not for samples that contain ≥ 5 wt% TiO_2, which includes 60603,10-16 and all high-Ti mare basalts. To date, no high-Ti impact melt sample has been identified in the lunar sample collections (Apollo, Luna, and lunar meteorites).

Conclusions: With regard to the olivine CSD from 60603,10-16, the distinct profile could be an extension of the impact melt field [6]. Indeed, the trace element chemistry would appear to support this, with the olivine analyses conducted as part of this study plotting in the impact melt field of [8] (Fig. 2). However, the whole rock composition of 60603,10-16 is high in TiO_2 (14.5 wt%; [1]) and [8] have shown that olivines from pristine high-Ti mare basalts tend to plot in the

impact melt field (see Fig. 2). As no high-Ti impact melts have been described from the Moon there is nothing to compare these data to so the origin of 60603,10-16 remains equivocal, but mineral geochemistry favors a picritic basalt origin.

While a CSD could not be constructed for olivine from 65703,9-13, their compositions indicate this sample is a pristine low-Ti mare basalt (Fig. 2), which further implies that the impact melt field of [6] does not extend above the Apollo 14 high-Al basalts.

References: [1] Zeigler, R.A. *et al.* (2006) *MaPS* **41**, 263-284. [2] Weiblen P. W. *et al.* (1974) *Proc. Lunar Conf. 5th* **1**, 749–767. [3] Dowty E. *et al.* (1974a) *Proc. Lunar Conf. 5th* **1**, 431–445. [4] Dowty E. *et al.* (1974b) *Earth Planet. Sci. Lett.* **24**, 15–25. [5] Korotev R. L. *et al.* (1997) *Geochim. Cosmochim. Acta* **61**, 2989–3002. [6] Donohue P. H. *et al.* (2013) *Abstracts of the Lunar and Planetary Science Conference* **44**, Abs. #2897. [7] Hui H. *et al.* (2011) *Geochim. Cosmochim. Acta* **75**, 6439–6460. [8] Fagan A. L. *et al.* (2013) *Geochim. Cosmochim. Acta* **106**, 429–445. [9] Roberts S. E. and Neal C. R. (2013) *LPSC 44*. [10] Neal C. R. *et al.* (2014) GCA (submitted). [11] Armstrong J. T. (1995) *Microbeam Analysis* **4**, 177–200. [12] Pearce N. J. *et al.* (1997) *Geostand. News.* **21**, 115–144. [13] van Achterbergh E. *et al.* (2001) Mineral. Assoc. Canada, Short Course Series **41**, 239–243.